Pulmonary Bronchiolar Cytotoxicity and Formation of Dichloroacetyl Lysine Protein Adducts in Mice Treated with Trichloroethylene

Poh-Gek Forkert, Brandie Millen, Lawrence H. Lash, David A. Putt and Burhan I. Ghanayem

Department of Anatomy and Cell Biology (P.-G.F., B.M.), Queen's University, Kingston, Ontario, Canada; Department of Pharmacology (L.H.L., D.A.P.), Wayne State University School of Medicine, Detroit, Michigan; and Laboratory of Pharmacology and Chemistry (B.I.G), National Institutes of Health, Research Triangle Park, North Carolina

1

Running title: Dichloroacetyl Lysine Protein Adducts in Murine Lung

Address correspondence to: Dr. Poh-Gek Forkert

Department of Anatomy and Cell Biology

Queen's University

Kingston, Ontario

Canada K7L 3N6

Phone: (613) 533-2854

Fax: (613) 533-2566

E-mail: forkertp@post.queensu.ca

Number of text pages: 31

Number of tables: 0

Number of figures: 7

Number of references: 37

Number of words in Abstract: 248

Number of words in Introduction: 756

Number of words in Discussion: 1474

Recommended section assignment: Toxicology

ABBREVIATIONS: CH, chloral hydrate; DASO$_2$, diallyl sulfone; DAL, dichloroacetyl lysine; PBS, phosphate-buffered saline; PNP, p-nitrophenol; SDS-PAGE, sodium dodecyl sulphate-polyacrylamide gel electrophoresis; TCE, trichloroethylene.

ABSTRACT

This study was undertaken to test the hypothesis that bronchiolar damage induced by trichloroethylene (TCE) is associated with bioactivation within the Clara cells with involvement of CYP2E1 and CYP2F2. Histopathology confirmed dose-dependent Clara cell injury and disintegration of the bronchiolar epithelium in CD-1 mice treated with TCE doses of 500 to 1000 mg/kg, i.p. Immunohistochemical studies, using an antibody that recognizes dichloroacetyl lysine adducts, revealed dose-dependent formation of adducts in the bronchiolar epithelium. Localization of dichloroacetyl adducts in the Clara cells coincided with damage to this cell type in TCE-treated mice. Pretreatment of CD-1 mice with diallyl sulfone, an inhibitor of CYP2E1 and CYP2F2, abrogated formation of the dichloroacetyl adducts and protected against TCE-induced bronchiolar cytotoxicity. Treatment of wild-type and CYP2E1-null mice with TCE (750 mg/kg, i.p.) also elicited bronchiolar damage that correlated with formation of adducts in the Clara cells. Immunoblotting, using lung microsomes from TCE-treated CD-1 mice, showed dose-dependent production of dichloroacetyl adducts that co-migrated with CYP2E1 and CYP2F2. However, TCE treatment resulted in loss of immunoreactive CYP2E1 and CYP2F2 proteins and p-nitrophenol hydroxylation, a catalytic activity associated with both P450 enzymes. The TCE metabolite, chloral hydrate, was formed in incubations of TCE with lung microsomes from CD-1, wild-type and CYP2E1-null mice. The levels were higher in CD-1 than in either wild-type or CYP2E1-null mice, although levels were higher in CYP2E1-null than in wild-type mice. These findings supported the contention that TCE bioactivation within the Clara cells, predominantly involving CYP2F2, correlated with bronchiolar cytotoxicity in mice.

Introduction

Trichloroethylene (C_2HCl_3; TCE) is a nonflammable, colorless liquid used extensively in vapor degreasing and cold cleaning of metal parts and as a result, occupational exposures are associated with the automotive, aviation and metals industries. It has been estimated that 3.5 million workers are exposed annually to TCE (NTP, 1990). Environmental release of TCE in the United States for the years 1988 to 1997 exceeded 345 million pounds (Toxics Release Inventory, 2004), leading to TCE becoming a major contaminant in soil and groundwater (ATSDR, 1997; 1999).

Exposure to TCE produces toxic effects in a variety of tissues including the liver, kidney, lung, nervous system and reproductive tissues. Available data are mostly derived from studies in the liver and showed that the toxicities produced by TCE are mediated via its biotransformation to reactive metabolites capable of binding to protein (Kautiainen et al., 1997; Cai and Guengerich, 2000). Other studies have identified the potential of TCE and its metabolites to induce T-cell activation and to promote autoimmunity (Gilbert et al., 2004). The metabolism of TCE is mediated through conjugative and oxidative pathways, and the selectivity of the specific pathway is related to the target organ. The conjugative pathway is a minor one and is associated with the nephrotoxic effects of TCE. Initial conjugation with glutathione, which takes place mainly in the liver, produces *S*-(1,2-dichlorovinyl)glutathione, and subsequent metabolic steps including transport and biotransformation result in formation of *S*-(1,2-dichlorovinyl)-L-cysteine, a metabolite linked to nephrotoxicity in rats (Bruning and Bolt, 2000; Dekant et al., 1990; Elfarra et al., 1986). The major route of TCE metabolism in the liver is oxidation via the cytochrome P450 system, and P450 enzymes including CYP2E1, CYP1A1/2, CYP2B1/2 and CYP2C11/6 have been implicated (Guengerich et al., 1991; Nakajima et al., 1990, 1992a, b). Chloral, TCE

4

oxide and dichloroacetyl chloride are initial metabolites generated from TCE oxidation.

Available evidence suggested that chloral and TCE oxide are both derived from an oxygenated

TCE-P450 intermediate (Miller and Guengerich, 1982; Cai and Guengerich, 2000). Chloral is

rapidly converted to chloral hydrate (CH) that then undergoes oxidation and reduction to form

trichloroacetic acid and trichloroethanol, respectively (Green and Prout, 1985; Dekant et al.,

1986). Dichloroacetyl chloride, which is believed to be derived from the TCE oxide, undergoes

decomposition to form dichloroacetic acid, but can also be formed from dechlorination of

trichloroacetic acid (Lash et al., 2000). Thus, TCE exposure and metabolism yields several

metabolites including chloral, CH, dichloroacetic acid, trichloroacetic acid, trichloroethanol and

dichloroacetyl chloride. Although the assignment of a TCE metabolite to a specific toxic effect

and/or to a specific tissue has proven to be a complex issue, it has been proposed that

trichloroacetic acid is associated with hepatotoxicity (Buben and O'Flaherty, 1985),

trichloroacetic acid and dichloroacetic acid with hepatocarcinogenicity (Bull et al., 2002), and *S*-

(1,2-dichlorovinyl)-L-cysteine with nephrotoxicity (Bruning and Bolt, 2000; Dekant et al., 1990).

An additional target of TCE is the lung where exposure causes lung cytotoxicity that is

manifested selectively in the Clara cells of the bronchiolar epithelium (Forkert et al., 1995).

Recent studies have implicated the P450 enzymes, CYP2E1, CYP2F2 and CYP2B1, in

bioactivation of TCE in murine lung (Forkert et al., 2005). Kinetic analysis using recombinant

P450 enzymes revealed that recombinant rat CYP2E1 metabolized TCE to CH with greater

affinity than did recombinant rat CYP2F4, recombinant mouse CYP2F2 and recombinant

CYP2B1. The catalytic efficiencies (V_{max}/K_m) for TCE metabolism followed the rank order

CYP2E1 > CYP2F4 > CYP2F2 > CYP2B1 (Forkert et al., 2005). These findings suggested that

CYP2E1 and CYP2F metabolized TCE to CH to the greatest extent, while CYP2B1 had a lesser

5

catalytic role. CYP2E1 and CYP2F2 are expressed constitutively in murine lung and since both are preferentially localized in the Clara cells (Forkert, 1995; Buckpitt et al., 1995), manifestation of cell damage in this cell type as a result of TCE exposure raises a question as to whether formation of reactive metabolites takes place within this cell type. Here, we have undertaken studies to test the hypothesis that bronchiolar epithelial damage is associated with TCE bioactivation within the Clara cells with involvement of CYP2E1 and CYP2F2. Immunochemical studies were carried out to determine formation of dichloroacetyl lysine (DAL) protein adducts, which were used as an in vivo marker of TCE metabolism. Our results showed that bronchiolar damage correlated with the formation of DAL protein adducts that were highly localized within the Clara cells. Furthermore, the findings suggested that bioactivation of TCE is mediated by CYP2E1 and CYP2F2, although CYP2F2 appears to have a more important role than CYP2E1 in the ensuing lung cytotoxicity in mice.

Materials and Methods

Chemicals and Reagents. Chemicals were purchased from suppliers as follows:

trichloroethylene (purity 99.5%), 4-nitrocatechol: Aldrich, Montreal, Quebec, Canada; sodium

pentobarbital (Somnotol): MTC Pharmaceuticals, Hamilton, Ontario, Canada; diallyl sulfone:

Colour Your Enzyme, Bath, ON, Canada; paraformaldehyde and hydrogen peroxide: Fisher

Scientific, Nepean, ON, Canada; avidin/biotin, streptavidin and rabbit anti-goat horseradish

peroxidase: Zymed, San Francisco, CA; goat anti-rabbit horseradish peroxidase, acrylamide/BIS,

polyvinylidene difluoride membrane, chemiluminescence reagents (Immuno-star HRP Substrate

kit), stripping buffer (Restore Western Stripping Buffer) and protein assay dye (BioRad,

Hercules, CA); goat anti-mouse horseradish peroxidase (Jackson ImmunoResearch, West Grove,

PA); bovine serum albumin, *p*-nitrophenol (PNP), 4-nitrocatechol, Ponceau S stain, 1,3-

dibromopropane, and goat anti-rabbit biotin (Sigma Chemical Co., St. Louis, MO); 3,3′-

diaminobenzidene tetrahydrochloride (DAKO, Carpinteria, CA). The anti-CYP2E1 polyclonal

antibody was obtained from Oxford Biomedical (Hornby, ON, Canada). The anti-dichloroacetyl

polyclonal antibody was donated by Dr. N. R. Pumford (University of Arkansas, Fayetteville,

Arkansas). The CYP2F1 antibody used as an analog for CYP2F2 was donated by Dr. G. S. Yost

(University of Utah, Salt Lake City, Utah), and has been shown in previous studies to cross-react

with CYP2F2 (Simmonds et al., 2004a).

Animal Treatment. Male CD-1 mice, weighing 25-28 g, were purchased from Charles

River Canada (St. Constant, QC, Canada). They were maintained on a 12 h light/dark cycle and

were provided with water and food (Mouse Diet 5015, PMI Nutrition International, Inc.,

Brentwood, MO) ad libitum. The mice were acclimatized to laboratory conditions for one week

before being used for experiments. For the histopathologic and immunohistochemical studies,

7

mice were treated with 500, 750 and 1000 mg/kg, i.p., of TCE in corn oil, and were sacrificed 4

h later. In the inhibition studies, mice were pretreated with diallyl sulfone (100 mg/kg) by

gavage, treated with TCE (750 mg/kg, i.p.) 2 h later and were sacrificed 4 h after TCE treatment.

The time of sacrifice was selected based on results from preliminary studies that showed

maximal labeling for DAL protein adducts in the bronchiolar epithelium at this time-point. In

the immunoblotting studies, mice were treated with 250, 500, 750 and 1000 mg/kg, i.p. of TCE

and were sacrificed 4 h later. In the experiments to determine PNP hydroxylation, mice were

treated with 50, 100, 250, 500, 750 and 1000 mg/kg (i.p.) of TCE and were sacrificed 4 h later.

Mice were anesthetized with sodium pentobarbital (120 mg/kg, i.p.), and lung tissue was fixed

and processed for immunohistochemistry and histopathology using methods described

previously (Forkert, 1995). In all experiments, control mice were treated with equivalent

volumes of vehicle.

Wild-type and CYP2E1-null mice were obtained from a colony (mixed 129/Sv and C57BL)

developed (Lee et al., 1996) at the National Cancer Institute (Bethesda, MD), and were re-

derived and bred at Charles River Laboratories, Inc. (Wilmington, MA). Male mice, weighing

22-35 g (2-3 months old) were quarantined at the National Institute of Environmental Health

Sciences (Research Triangle Park, NC) for one week before use in temperature- and humidity-

controlled rooms with a 12-h light/dark cycle. National Institutes of Health 31 rodent chow diet

and tap water were provided ad libitum. All animal care and experimental procedures were

performed according to the National Institutes of Health guidelines (NIH, 1985).

Histopathology. Lungs were fixed by tracheal instillation and vascular perfusion using

procedures described previously (Forkert, 1995). Briefly, a cannula was inserted into the right

ventricle and lung tissue was flushed with saline. Following removal of excess blood from the

8

tissue, lungs were perfused with 4% paraformaldeyde in 0.1 M Sorensen's phosphate buffer

(12.0 mM NaH_2PO_4, 69.0 mM Na_2HPO_4), pH 7.4. The lungs were also inflated with 0.3 ml of

the fixative. Tissues were fixed overnight and were then dehydrated, cleared and embedded in

paraffin using standard procedures. Paraffin sections (5 μm) were prepared from lung tissue and

were stained with hematoxylin and eosin for histopathologic observation by light micrsoscopy.

Immunohistochemical Localization of DAL Protein Adducts. Lung tissue was fixed as

described for histopathology. Paraffin sections (5 μm) were prepared and adhered to glass

slides. Identification of DAL proteins in tissue sections was performed using an anti-DAL

antibody (1:500) and the avidin-biotin complex technique. The sections were deparaffinized,

cleared and hydrated in a graded ethanol series. The sections were rinsed in phosphate-buffered

saline (PBS), and treated with 5% normal goat serum to block nonspecific antibody binding.

The sections were then incubated for 60 min with the anti-DAL antibody (1:200) diluted in PBS

containing 2.5% normal goat serum. After thorough rinsing in PBS, tissue sections were reacted

for 30 min with a biotinylated goat anti-rabbit antibody. Endogenous peroxidase activity was

inhibited by incubating tissue sections with 1% hydrogen peroxide in water for 30 min. Sections

were then reacted for 10 min with streptavidin conjugated to horseradish peroxidase, and the

immunoperoxidase color reaction developed by reaction with 0.05% 3,3'-diaminobenzidine

tetrahydrochloride and 0.01% hydrogen peroxide. The sections were then rinsed, incubated for 5

min in 0.15 M sodium chloride containing 0.5% copper sulfate, dehydrated, cleared, and

mounted. Controls for the specificity of the immunohistochemical reactions included

incubations performed in the absence of the anti-DAL antibody.

Preparation of Microsomes. Lung tissues from 30 mice were pooled for each lung

microsomal sample. Microsomes were prepared by differential centrifugation as described

previously (Simmonds et al., 2004b), with minor modifications. Lung tissue was minced and

homogenized in 4 volumes of cold phosphate-buffered KCl (139 mM KCl, 100 mM K_2HPO_4,

1.5 mM EDTA, pH 7.4). The homogenate was subjected to centrifugation at 12,000g for 20 min

at 2°C. The supernatant was then centrifuged at 105,000g for 60 min. The pellet was

homogenized using three strokes of the pestle and the resulting homogenate was centrifuged at

12,500g for 60 min. The final pellet was homogenized using 400 μl of buffer and a hand-held

pestle. Microsomes were also prepared from the lungs of wild-type and CYP2E1-null mice;

tissues from 30 mice each were pooled for each microsomal sample. Aliquots of lung

microsomes were frozen in liquid nitrogen and stored at -70°C. Microsomal protein

concentrations were determined by the dye binding protein assay, using bovine serum albumin as

the standard.

Protein Immunoblotting. Protein blots were prepared using a modification of procedures

described previously (Forkert, 1995). Microsomal proteins were separated by SDS-PAGE, using

an 8.5 % gel, and were then transferred to a polyvinylidene difluoride membrane. Microsomal

proteins from human β-lymphoblastoid cells containing a CYP2F1 insert were included to serve

as a positive control for the CYP2F2 protein. Low-range SDS-PAGE standards (BioRad,

Hercules, CA) were included with each gel. Next, the membrane was stained with Ponceau S

(Sigma Chemical Co., St. Louis, MO) to confirm uniform protein loading and transfer to the

membrane. The membrane was incubated overnight in a blocking solution consisting of 10%

non-fat milk powder in 20 mM Tris-HCl containing 500 mM NaCl, pH 7.5. After rinsing, the

membrane was incubated for 2 h with a CYP2F1, CYP2E1 or anti-DAL antibody. The CYP2F1

antibody was affinity purified using a SulfoLink Coupling gel kit (Pierce Chemical, Rockford,

IL) and the anti-DAL antibody was purified using an Immunopure IgG purification kit (Pierce

Chemical, Rockford, IL). The blots were incubated in a horseradish-peroxidase conjugated secondary antibody for 2 h as follows: CYP2F1 and anti-DAL with goat-anti-rabbit-IgG (1:18 000) and CYP2E1 with rabbit-anti-goat-IgG (1:5 000). The protein bands were visualized using chemiluminescence reagents (Immuno-Star™ HRP Substrate Kit, BioRad, Hercules, CA). The blots were then stripped using Restore Western Stripping buffer (Pierce Chemical, Rockford, IL) for 15 min at 37°C. Initially, the efficiency of the stripping was assessed by incubating the membrane with the goat anti-rabbit IgG conjugated to horseradish peroxidase (1:1 500) and reacting with the chemiluminescence detection reagents. The absence of protein bands indicated that the stripping was successful. The stripped membrane was incubated overnight at 4°C with the CYP2E1 polyclonal antibody (1:500), the CYP2F1 polyclonal antibody (1:1 500) or the anti-DAL antibody (1:500). After rinsing in T/TBS, the membrane was incubated for 2 h with a rabbit anti-goat antibody conjugated to horseradish peroxidase. The protein bands were visualized by reaction with chemiluminescence detection reagents. Densitometric scanning and analysis of the protein bands in the gels were performed using Kodak 1D Image Analysis Software (Sigma-Aldrich Corp., St. Louis, MO).

Enzyme Assays. Hydroxylation of PNP was used as a marker for both CYP2E1 and CYP2F2 catalytic activity (Shultz et al., 1999; Simmonds et al., 2004a). Reaction mixtures contained lung microsomal proteins (0.5 mg) from mice treated with TCE (50-1000 mg/kg, i.p.) and NADPH (1.5 mM). After preincubation for 3 min at 37°C, PNP (1 mM) in dimethyl sulfoxide was added, and the incubations were continued for an additional 10 min. Microsomal proteins were precipitated with perchloric acid (70%, 20 µl) and removed by centrifugation. Quantification of PNP in the supernatant fraction was determined by HPLC analysis as described previously (Duescher and Elfarra, 1993). Briefly, samples (100 µl) were analyzed using a

11

Beckman System Gold Programmable Solvent Module 126 HPLC, a reversed-phase C_{18} column

(5 µm, 4.6 x 250 mm; Beckman Ultrasphere ODS) and a Beckman System Gold Module 168 UV

detector. The isocratic mobile phase was 25% acetonitrile: 75% H_2O:0.1% trifluoroacetic acid

with a flow rate of 1.5 ml/min. The column effluent was monitored at 345 nm. Levels of PNP

hydroxylase activity were assessed by formation of 4-nitrocatechol, which eluted from the

column at 5.5 min, and quantified by relating peak area to a standard calibration curve of known

amounts of 4-nitrocatechol.

Formation of Chloral Hydrate in Lung Microsomal Incubations. Reaction mixtures in a

total volume of 500 µl of 50 mM Tris-HCl buffer, pH 7.4, consisted of lung microsomal proteins

(0.25 mg) from untreated mice, NADPH (1.0 mM) and TCE (0.25 - 5 mM) in acetonitrile (0.4%,

v/v). The incubations were performed at $37^{o}C$ for 20 min and the reactions were terminated by

freezing in liquid nitrogen. Detection of CH was determined using the method described

previously (Cummings et al., 2001). Samples (250 µl) were thawed and extracted with ethyl

acetate (0.5 ml) after which 1,2-dibromopropane (10 nmol) was added as an internal standard.

Analysis for TCE and CH was performed by gas chromatography with electron capture

detection, using a Perkin-Elmer PE-210 capillary column (30 m x 0.25 mm I.D. x 0.5 µm film

thickness) and a Perkin-Elmer AutoSystem XL GC system. Injector temperature was 200˚C,

detector temperature was 300˚C, and He was the carrier at a flow rate of 24.8 ml/min at 150˚C.

Oven temperature was maintained at $35^{o}C$ for 11 min followed by a linear increase from 35 to

$120^{o}C$ in 8 min with a final holding temperature of 120˚C for a further 19 min. Retention times

for TCE and CH were 3.90 and 6.15 min, respectively. Limits of detection were 0.2 and 0.05

pmol per mg protein for TCE and CH, respectively.

Results

Histopathology. The bronchiolar epithelium in control CD-1 mice contained numerous Clara cells with normal characteristics (Fig. 1A). In mice treated with 500 mg/kg (i.p.) of TCE, structural alterations at 4 h consisted of a few Clara cells with pyknotic nuclei that were in the process of exfoliation (Fig. 1B). The epithelial injury was exacerbated after exposure to a TCE dose of 750 mg/kg and was characterized by disruption of the epithelium; the Clara cells appeared distorted, were sloughed or were in the process of losing their apices (Fig. 1C). Treatment of mice with 1000 mg/kg produced more severe cytotoxicity with segments of the bronchiole that were denuded of epithelium and with exfoliated epithelial cells present in the airway lumen (Fig. 1D). Damage was not apparent in the alveolar type II cells following treatment with any TCE dose.

In the inhibitory studies, treatment of CD-1 mice with TCE (750 mg/kg, i.p.) alone exhibited morphologic features indicative of distintegration as in the histopathologic studies described previously (Figs. 3A and 1C). In CD-1 mice that were pretreated with DASO$_2$ 2 h before TCE treatment, the bronchiolar epithelium appeared intact and contained numerous Clara cells that exhibited normal characteristics (Figs. 3E and 1C).

In CYP2E1-null mice treated with 750 mg/kg of TCE, many Clara cells appeared to have undergone exfoliation and/or lost their apices so that the residual epithelium appeared flattened and markedly less substantial than in untreated mice (Fig. 3E). The extent of damage in CYP2E1-null mice was slightly more severe than in wild-type mice treated with the same TCE dose (not shown). The Clara cell lesion was also more severe in CYP2E1-null than in CD-1 mice treated with the 750 mg/kg TCE dose (Figs. 1C and 4A).

Localization of DAL Protein Adducts. Immunohistochemical studies were performed on lung tissue sections from TCE-treated CD-1, wild-type and CYP2E1-null mice. A polyclonal anti-DAL antibody was used for these studies. Positive labeling for the DAL protein adducts was observed in the bronchiolar epithelium of CD-1 mice (Fig. 2). The labeling was prominent in the Clara cells and was concentrated within their cellular apices (Fig. 2, B and C). The extents of labeling were dose-dependent and were more abundant in lung sections from mice treated with 1000 mg/kg of TCE (Fig. 2D) than in those treated with doses of 500 and 750 mg/kg (Fig. 2, B and C). Dose-dependent formation of the protein adducts was also found in alveolar type II cells (Fig. 2, B-D). The labeling was not visualized in lung sections from untreated mice reacted with the anti-DAL antibody (Fig. 2A) or in sections from TCE-treated mice that were not reacted with the anti-DAL antibody (not shown).

In the inhibition studies, labeling for the DAL protein adducts was seen in the bronchiolar epithelium and Clara cells of CD-1 mice treated with only TCE (750 mg/kg, i.p.) (Fig. 3C). In mice pretreated with $DASO_2$ 2 h before TCE treatment, immunoreactivity for the DAL adducts was minimal and was similar to that in untreated mice (Fig. 3D).

Labeling was not observed in lung tissue from either wild-type or CYP2E1-null mice that were untreated (not shown). In CYP2E1-null mice treated with TCE (750 mg/kg), labeling for the DAL adducts was observed in the bronchiolar epithelium, but the immunoreactivity appeared less pronounced than in CD-1 mice treated with the same TCE dose, due in part to attenuation of the epithelium and loss of Clara cells in the null mice (Fig. 3F). The labeling was also seen in the lungs of TCE-treated wild-type mice (not shown).

Protein Immunoblotting. Protein blots were prepared with lung microsomal proteins from mice treated with various doses of TCE (250, 500, 750 and 1000 mg/kg). The anti-DAL

14

antibody detected a major protein band of about 51 kDa in the lung microsomal proteins (Fig. 4A). The immunoreactivities of the DAL protein adducts were dose-dependent and were incremental with microsomal proteins from mice treated with increasing doses of TCE. When the blot was stripped and subsequently re-probed with a CYP2E1 antibody, a protein band of 51 kDa was also visualized (Fig. 4B). Immunodetectable CYP2E1 protein was highest in lung microsomes from untreated mice but was virtually abolished in microsomes from mice treated with all TCE doses (Fig. 4B). Staining with Ponceau S showed that loading of microsomal proteins from mice subjected to different treatment regimens was similar (Fig. 4C).

Additional protein blots were prepared with lung microsomal proteins from control and TCE-treated mice, using the anti-DAL antibody. The DAL protein adducts were visualized as a band with a molecular mass of 56 kDa, and confirmed to have dose-dependent immunoreactivities in mice treated with TCE doses ranging from 250 to 1000 mg/kg (Fig. 5A). Loading of the microsomal proteins, as assessed by Ponseau S staining, was comparable in all the lung samples (Fig. 5C). When the blots were stripped and reacted with the anti-CYP2F1 antibody, CYP2F2 was recognized as a protein band of about 56 kDa, although the control consisting of β-lymphoblastoid microsomes containing a CYP2F1 insert migrated at a slightly more rapid rate than the CYP2F2 protein (Fig. 5B). The CYP2F2 protein was present in lung microsomes from untreated mice (Fig. 5B). However, treatment of mice with TCE resulted in loss of immunodetectable CYP2F2 protein in lung microsomes from mice treated with doses of TCE ranging from 250 to 1000 mg/kg (Fig. 5B).

Microsomal PNP Hydroxylation. Treatment of mice with 50 mg/kg TCE caused a precipitous decline to 63% of control in lung microsomal PNP hydroxylase activity (Fig. 6). Further decreases of 76% and 80% were detected when mice were treated with TCE at doses of

100 and 250 mg/kg, respectively. The nadir was reached at 500 mg/kg when residual levels

comprised only 8% of the control level. No further decreases in hydroxylase activity were

observed at TCE doses of 750 or 1000 mg/kg. There was no loss of enzyme activity in lung

microsomes from control mice treated with corn oil.

Formation of Chloral Hydrate in Lung Microsomal Incubations. Formation of CH was

determined in incubations of TCE with lung microsomes from male CD-1, wild-type and

CYP2E1-null mice. In CD-1 mice, rates of CH production were linear in microsomal

incubations containing 0.25 to 3.0 mM TCE (Fig. 7A). Saturation was achieved at 3.0 mM as no

further increase in the rates of CH formation was found in incubations containing 5.0 mM of

TCE. In wild-type and CYP2E1-null mice, the rates of CH formation were almost identical in

microsomal incubations containing 0.25 to 0.75 mM TCE (Fig. 7B). However, the rates of CH

production differed in wild-type and CYP2E1-null mice at higher TCE concentrations. The peak

rates of CH formation in wild-type mice were achieved at a TCE concentration of 0.75 mM, with

declines occurring at concentrations of 1.0 and 2.0 mM. In CYP2E1-null mice, peak rates of CH

formation were achieved at 1.0 mM of TCE and were lower in incubations containing a

concentration of 2.0 mM. A plateau in the rates of CH formation in lung microsomes from wild-

type and CYP2E1-null mice was observed in incubations with TCE concentrations of 2.0 to 5.0

mM. Hence, saturation in the rates of CH production in wild-type mice (0.75 mM) occurred at a

lower TCE concentration than in CYP2E1-null mice (1.0 mM), and both concentrations were

substantially lower than for CD-1 mice (3.0 mM). Formation of CH was absent or minimal in

control incubations performed in the absence of NADPH or TCE.

Discussion

The vulnerability of the Clara cells to chemically-induced cytotoxicity has been ascribed to their substantial content of cytochrome P450 enzymes capable of mediating the bioactivation of substrates to reactive metabolites that elicit cellular toxicities. Early studies have identified Clara cell and bronchiolar cytotoxicity in mice treated with TCE (Forkert et al., 1985). More recent studies have yielded data supporting involvement of CYP2E1, CYP2F2 and CYP2B1 in mediating TCE metabolism to CH (Forkert et al., 2005). Since CYP2E1 and CYP2F2 are highly concentrated in the Clara cells (Forkert, 1995; Buckpitt et al., 1995), we postulated that bioactivation of TCE takes place within the target cell population leading to the selective damage of the Clara cells. The formation of DAL protein adducts was used as an in vivo marker of TCE metabolism, and was identified immunochemically using an antiserum directed against dichloracetic anhydride-modified rabbit serum albumin (Halmes et al., 1996; Griffin et al., 1998). Binding of the antibody to TCE adducts on immunoblots of liver microsomes was completely inhibited by N^ϵ-(dichloroacetyl)-L-lysine, indicating that the antibody recognized DAL residues on proteins. The formation of N^6-(dichloroacetyl)lysine from TCE metabolism has been confirmed in studies using liver microsomal incubations and bovine serum albumin as the model protein (Cai and Guengerich, 2000). Our immunohistochemical studies in TCE-treated CD-1 mice showed formation of DAL protein adducts that were highly localized in the Clara cells of the bronchiolar epithelium (Fig. 2). The formation of the DAL protein adducts was dose-dependent as the magnitudes of labeling were incremental in mice treated with 500 to 1000 mg/kg of TCE (Fig.2, B-D). The severities of Clara cell damage were dose-dependent, and were most pronounced in mice treated with 1000 mg/kg of TCE (Fig. 1F). In CYP2E1-null mice treated with 750 mg/kg of TCE, labeling for the DAL protein adducts was also highly localized

in the bronchiolar epithelium and in the Clara cells (Fig. 3F), and coincided with damage to this cell type (Fig. 3E). These results affirmed the coincidental localization of DAL protein adducts and cell damage in the bronchiolar epithelium, and supported the assumption that the cytotoxic effects are mediated via TCE metabolism within the target Clara cells. However, it should be noted that dose-dependent formation of DAL protein adducts was also found in alveolar type II cells (Fig. 2, B-D), although cell injury was not apparent. This observation suggested that there may be a threshold in adduct formation and hence bioactivation at which toxicity is manifested.

The dose-dependent formation of DAL protein adducts in the lungs of CD-1 mice indicated that dichloroacetyl chloride was generated from TCE in this tissue. Moreover, there was dose-dependent production of CH in incubations of CD-1 lung microsomes with TCE (Fig. 7A). A question arises regarding which TCE metabolite(s) represents the reactive species. It has been proposed that accumulation of chloral within the Clara cells is responsible for their susceptibility to TCE-induced cytotoxicity (Odum et al., 1992). This accumulation has been ascribed to diminished metabolism of chloral to trichloroethanol and its glucuronide. Furthermore, treatment of mice with chloral produced a Clara cell lesion similar to that induced by TCE. Other studies have shown that while murine lung microsomes were able to metabolize TCE to chloral at a significant rate, the rate in rat lung was 23-fold lower (Green et al., 1997). It has been proposed that the differing capabilities for chloral formation in mice and rats are associated with the development of lung tumors in mice but not in rats exposed to TCE by inhalation (Green, 2000; Fukuda et al., 1983: Maltoni et al., 1986). Although plausible, direct evidence for this proposed mechanism is lacking. However, our finding of relatively more severe bronchiolar damage in CYP2E1-null mice (Figs. 3E) coupled with diminished rates of CH formation (Fig. 7) compared to those in CD-1 mice argues against chloral as the proximate toxicant. Whether

dichloroacetyl chloride and/or other metabolite(s) play a pertinent role in TCE-induced lung

cytotoxicity and/or carcinogenicity remains to be established. In the context of carcinogenicity,

it is of interest to identify the cell of origin of the lung tumors to verify if it coincides with the

cell type in which TCE bioactivation takes place.

Previous studies have reported that a reactive intermediate formed from TCE metabolism

binds to a 50 kDa protein in murine liver that has been postulated to be CYP2E1 (Griffin et al.,

1998). A subsequent investigation using rat hepatocytes exposed to TCE demonstrated the

presence of a similar 50 kDa protein that co-migrated with CYP2E1 (Griffin et al., 1998). This

50 kDa protein was not detected in human hepatocytes but instead a 47 kDa protein that did not

co-migrate with CYP2E1 was identified, suggesting that the P450 isoforms that metabolized

TCE differs in rats vs. humans. These data suggested that TCE metabolism by CYP2E1

produces a dichloroacetyl metabolite that binds to the CYP2E1 apoprotein at the site of

formation. In this investigation, studies were performed to further explore this concept in murine

lung. Since CYP2E1 and CYP2F2 mediated bioactivation of TCE in the lung, formation of a

reactive species that binds to the apoprotein moieties of these P450 enzymes should generate

protein adducts with gel mobilities similar to those for CYP2E1 and CYP2F2, although it is

probable that multiple proteins may exhibit similar gel mobilities. Immunoblots prepared using

lung microsomes and the anti-DAL antibody demonstrated that TCE treatment yielded protein

bands of 51 kDa exhibiting dose-dependent immunoreactivities for doses ranging from 250 to

1000 mg/kg (Figs. 4 and 5). When the blots were stripped and reprobed with either an anti-

CYP2E1 or an anti-CYP2F1 antibody, immunodetectable protein bands corresponding to those

for the DAL adducts were visualized (Figs. 4 and 5). In both cases, CYP2E1 and CYP2F2 were

constitutively expressed and TCE treatment caused loss of protein content of both P450

enzymes, indicating treatment-related modification of CYP2E1 and CYP2F2 protein structures. These findings suggested that a reactive TCE metabolite including dichloroacetyl chloride was formed capable of binding to both P450 proteins and rendering the epitopes unrecognizable by the antibody. Moreover, the P450 enzymes were catalytically inactivated, as there was dose-dependent loss of PNP hydroxylation, an enzyme catalytic activity shown to be associated with both CYP2E1 and CYP2F2 (Shultz et al., 1999; Simmonds et al., 2004a). The involvement of CYP2E1 and CYP2F2 is supported by the results of in vivo inhibitory studies with $DASO_2$, a garlic compound that has been shown to inhibit CYP2E1 and CYP2F2 (Simmonds et al., 2004a. Pretreatment of mice with $DASO_2$ 2 h before TCE inhibited the formation of DAL protein adducts and protected from bronchiolar cytotoxicity (Fig. 3, A and B). Taken together, these findings are consistent with a role for CYP2E1 and CYP2F2 in TCE metabolism in murine lung.

Previous studies using recombinant P450 enzymes suggested that CYP2E1 is a major isoform mediating TCE metabolism (Forkert et al., 2005). On the basis of these findings, we postulated that treatment of CYP2E1-null mice with TCE should result in diminution of both bronchiolar cytotoxicity and production of DAL adducts, compared with the effects in wild-type mice. In addition, incubations of TCE with lung microsomes from CYP2E1-null mice should result in decreased rates of CH production indicative of reduced TCE metabolism. Surprisingly, our results showed that bronchiolar damage and formation of DAL protein adducts were undiminished in the lungs of CYP2E1-null mice (Fig. 3, E and F). Moreover, generation of CH from TCE in incubations of lung microsomes from CYP2E1-null mice were achieved at rates that were higher than in wild-type mice (Fig. 7B). These findings suggested that CYP2F2 has a more important role than CYP2E1 in TCE metabolism in murine lung, and these data differed from those derived from studies using recombinant P450 enzymes (Forkert et al., 2005).

20

Recombinant rat CYP2E1 (V_{max} /K_m = 0.79) demonstrated greater catalytic affinity and

efficiency for TCE metabolism than did recombinant CYP2F2 (V_{max} /K_m = 0.11), suggesting that

TCE metabolism in rats and mice may differ, and may be mediated mainly by CYP2E1 in rats

and CYP2F2 in mice. However, the higher rates of CH production by lung microsomes from

CYP2E1-null mice compared to rates in wild-type mice may not be mediated entirely by

CYP2F2. Compensatory up-regulation of P450 enzymes involved in TCE metabolism and/or

recruitment of other P450 enzymes might also be responsible for the outcome in the lungs of

CYP2E1-null mice. In this regard, studies of protein content and catalytic activities of CYP2E1

and CYP2F2 as well as of other P450 enzymes in wild-type and CYP2E1-null mice are

particularly called for to characterize their metabolic status under conditions of gene disruption.

In summary, the results of this study are consistent with the contention that bronchiolar

damage induced by TCE is associated with its bioactivation within the target Clara cells.

Furthermore, the findings supported the involvement of CYP2E1 and CYP2F2 in TCE

metabolism, although CYP2F2 appears to have a more important role than CYP2E1 in murine

lung.

Acknowledgments

References

ATSDR (Agency for Toxic Substances and Disease Registry, Division of Toxicology) (1997) Toxicological profile for trichloroethylene (update). ATSDR, Atlanta, GA.

ATSDR (Agency for Toxic Substances and Disease Registry) (1999) National Exposure Registry, Trichloroethylene Subregistry Baseline through Followup-3 Technical Report. U.S. Department of Health and Human Services, Public Health Service, Atlanta, GA.

Bruning T and Bolt HM (2000) Renal toxicity and carcinogenicity of trichloroethylene: key results, mechanisms, and controversies. *Crit Rev Toxicol* **30**:253-285.

Buben JA and O'Flaherty EJ (1985) Delineation of the role of metabolism in the hepatotoxicity of trichloroethylene and perchloroethylene: a dose-effect study. *Toxicol Appl Pharmacol* **78**:105-122.

Buckpitt A, Chang A, Weir A, Van Winkle L, Duan X, Philpot RM and Plopper CG (1995) Relationship of cytochrome P450 activity to Clara cell cytotoxicity. IX. Metabolism of naphthalene and naphthalene oxide in microdissected airways from mice, rats and hamsters. *Mol Pharmacol* **47**:74-81.

Bull RJ, Orner GA, Cheng RS, Stillwell L, Stauber AJ, Sasser LB, Lingohr MK and Thrall BD (2002) Contribution of dichloroacetate and trichloroacetate to liver tumor induction in mice by trichloroethylene. *Toxicol Appl Pharmacol* **182**:55-65.

Cai H and Guengerich FP (2000) Acylation of protein lysines by trichloroethylene oxide. *Chem Res Toxicol* **13**:327-335.

Cummings BS, Parker JC and Lash LH (2001) Cytochrome P-450-dependent metabolism of trichloroethylene in rat kidney. *Toxicol Sci* **60**:11-19.

Dekant W, Koob M and Henschler D (1990) Metabolism of trichloroethene – in vivo and in vitro evidence for activation by glutathione conjugation. *Chem-Biol Interact* **73**:89-101.

Dekant W, Schultz A, Metzler M and Henschler D (1986) Absorption, elimination and metabolism of trichloroethylene: a quantitative comparison between rats and mice. *Xenobiotica* **16**:143-152.

Duescher RJ and Elfarra AA (1993) Determination of *p*-nitrophenol hydroxlase activity of rat liver microsomes by high-pressure liquid chromatography. *Anal Biochem* **212**:311-314.

Elfarra AA, Jacobson I and Anders MW (1986) Mechanism of *S*-(1,2-dichlorovinyl)glutathione-induced nephrotoxicity. *Biochem Pharmacol* **35**:283-288.

Forkert PG (1995) CYP2E1 is preferentially expressed in Clara cells of murine lung: localization by *in situ* hybridization and immunohistochemical methods. *Am J Resp Cell Mol Biol* **12**: 589-596.

Forkert PG, Baldwin RM, Millen B, Lash LH, Putt DA, Shultz MA and Collins KS (2005) Pulmonary bioactivation of trichloroethylene to chloral hydrate: relative contributions of CYP2E1, CYP2F and CYP2B1. *Drug Metab Dispos* **33**:1429-1437.

Forkert PG, Sylvestre PL and Poland, JS (1985) Lung injury induced by trichloroethylene. *Toxicology* **35**:143-160.

Fukuda K, Takemoto K and Tsurata H (1983) Inhalation carcinogenicity of trichloroethylene in rats and mice. *Ind Health* **21**:243-254.

Gilbert KM, Whitlow AB and Pumford NR (2004) Environmental contaminant and disinfection by-product trichloroacetaldehyde stimulates T cells in vitro. *Internat Immunopharmacol* **4**:25-36.

Green T (2000) Pulmonary toxicity and carcinogenicity of trichloroethylene: species differences
and mode of action. *Environ Health Perspect* **108 (suppl 2)**:261-264.

Green T, Mainwaring GW and Foster JR (1997) Trichloroethylene-induced mouse lung tumors:
studies of the mode of action and comparisons between species. *Fund Appl Toxicol* **37**:125-
130.

Green T and Prout MS (1985) Species differences in response to trichloroethylene. II.
Biotransformation in rats and mice. *Toxicol Appl Pharmacol* **79**:401-411.

Griffin JM, Lipscomb JC and Pumford NR (1998) Covalent binding of trichloroethylene to
proteins in human and rat hepatocytes. *Toxicol Letts* **95**:173-181.

Guengerich FP, Kim D-H, and Iwasaki M (1991) Role of human cytochrome P-450 IIE1 in the
oxidation of many low molecular weight cancer suspects. *Chem Res Toxicol* **4**:168-179.

Halmes NC, McMillan DC, Oatis, Jr., JE, and Pumford NR. Immunochemical detection of
protein adducts in mice treated with trichloroethylene. *Chem Res Toxicol* **9**:451-456, 1996.

Kautiainen A, Vogel JS and Turteltaub KW (1997) Dose-dependent binding of trichloroethylene
to hepatic DNA and protein at low doses in mice. *Chem-Biol Interact* **106**:109-121.

Lash LH, Fisher JW, Lipscomb JC and Parker JC (2000) Metabolism of trichloroethylene.
Environ Health Perspect **108 (suppl 2)**:177-2000.

Lee SS, Pineau T, Fernandez-Salguero P, and Gonzalez FJ (1996) Role of CYP2E1 in the
hepatotoxicity of acetaminophen. *J Biol Chem* **271**:12063-12067.

Maltoni C, Lefemine G, Cotti G and Perino G (1986) Long-term carcinogenicity bioassays on
trichloroethylene administered by inhalation in Sprague-Dawley rats and Swiss and B6C3F1
mice. *Ann NY Acad Sci* **534**:316-342.

Miller RE, and Guengerich FP (1982) Oxidation of trichloroethylene by liver microsomal cytochrome P-450: evidence for chlorine migration in a transition state not involving trichloroethylene oxide. *Biochemistry* **21**:1090-1097.

Nakajima T, Wang R-S, Muruyama N and Sato A (1990) Three forms of trichloroethylene-metabolizing enzymes in rat liver induced by ethanol, phenobarbital, and 3-methylcholanthrene. *Toxicol Appl Pharmacol* **102**:546-552.

Nakajima T, Wang R-S, Elovaara E, Park SS, Gelboin HV and Vainio H (1992a) A comparative study of the contribution of cytochrome P450 isozymes to metabolism of benzene, toluene and trichloroethylene in rat liver. *Biochem Pharmacol* **43**:251-257.

Nakajima T, Wang R-S, Katakura Y, Kishi R, Elovaara E, Park SS, Gelboin HV and Vainio H (1992b) Sex-, age-, and pregnancy-induced changes in metabolism of toluene and trichloroethylene in rat liver in relation to the regulation of cytochrome P450IIIE1 and P450IIC11 content. *J Pharmacol Exp Ther* **261**:869-874.

NIH (National Institutes of Health) (1985) Guide for the care and use of laboratory animals. U.S. Department of Health and Human Services, Animal Resources Program, Division of Resources, Bethesda, MD.

NTP (1990) Carcinogenesis studies of trichloroethylene (without epichlorohydrin) in F344/N rats and BC63F1 mice (gavage study). NTP Tech. Rep. 243, CAS No. 79-01-06. National Toxicology Program, Research Triangle Park, NC.

Odum J, Foster JR and Green T (1992) A mechanism for the development of Clara cell lesions in the mouse lung after exposure to trichloroethylene. *Chem-Biol Interact* **83**:135-153.

Shultz MA, Choudary PV, and Buckpitt AR (1999) Role of murine cytochrome P-450 2F2 in

metabolic activation of naphthalene and metabolism of other xenobiotics. *J Pharmacol Exp

Ther* **290**:281-288.

Simmonds AC, Ghanayem BI, Sharma A, Reilly CA, Millen B, Yost GS, and Forkert PG

(2004a) Bioactivation of 1,1-dichloroethylene by CYP2E1 and CYP2F2 in murine lung. *J

Pharmacol Exp Ther* **310**:855-864.

Simmonds AC, Reilly CA, Baldwin RM, Ghanayem BI, Lanza DL, Yost GS, Collins KS and

Forkert PG (2004b) Bioactivation of 1,1-dichloroethylene to its epoxide by CYP2E1 and

CYP2F enzymes. *Drug Metab Dispos* **32**:1032-1039.

Toxics Release Inventory (2004) U.S. Environmental Protection Agency.

http://www.epa.gov/triexplorer/ Accessed: March 2004.

Footnotes

b) Address correspondence to: Dr. Poh-Gek Forkert, Department of Anatomy and Cell Biology,

    Queen's University, Kingston, ON, Canada K7L 3N6. E-mail:forkertp@post.queensu.ca

Figure Legends

Fig. 1. Histopathology of bronchiolar epithelium in the lungs of TCE-treated CD-1 mice. Mice were treated with corn oil (A) or TCE at doses of 500 (B), 750 (C) or 1000 (D) mg/kg, i.p., and were sacrificed 4 h later. Clara cells (arrowheads) appear normal in control mice (A). In mice treated with 500 mg/kg, pyknotic Clara cells (arrowheads) are becoming detached (B). Treatment with 750 mg/kg of TCE produced attenuation of the bronchiolar epithelium due to exfoliation and/or loss of Clara cell apices (arrowhead). Treatment with 1000 mg/kg resulted in denudation of portions of the epithelium (arrowhead) and the presence of exfoliated cells in the airway lumen (arrow). Tissue sections were stained with hematoxylin and eosin. Scale bars: 20 μm.

Fig. 2. Localization and distribution of DAL protein adducts in lung tissue of CD-1 mice. Immunohistochemical labeling was performed using a rabbit anti-DAL polyclonal antibody and the avidin-biotin complex procedure. Labeling for the protein adducts was absent in control mice (A), but was localized in the bronchiolar epithelium of TCE-treated mice. The labeling was incremental with TCE doses of 500 (B), 750 (C) and 1000 (D) mg/kg. Insets in panel B and C depict localization of DAL protein adducts in the Clara cells and their concentration in the cell apices (arrowheads). Scale bars: 20 μm.

Fig. 3. Effect of TCE (750 mg/kg, i.p.) treatment on histopathology and localization of DAL protein adducts in the lungs of CYP2E1-null mice (E and F) and in CD-1 mice pretreated with DASO$_2$ (100 mg/kg, p.o.) (A-D). In TCE-treated CD-1 mice, the bronchiolar epithelium appeared attenuated and the airway lumen contained detached epithelial cells (arrowheads) (A). In CD-1 mice pretreated with DASO$_2$, the bronchiolar epithelium contained normal Clara cells (arrowheads) (B). Labeling for DAL protein adducts in CD-1 mice was concentrated in the

29

bronchiolar epithelium (C) and was absent in mice pretreated with DASO$_2$ (D). In TCE-treated

CYP2E1-null mice, Clara cells were damaged, resulting in flattening of the epithelium (arrow)

and the presence of cell debris in the airway lumen (arrowheads) (E). Labeling for DAL protein

adducts was localized in the bronchiolar epithelium and in residual Clara cells (arrowheads) (F).

Tissue sections for histopathology were stained with hematoxylin and eosin, and

immunohistochemistry was performed using an anti-DAL polyclonal antibody and the avidin-

biotin complex procedure. Scale bars: 20 μm (A-D and F); .

Fig. 4. Effect of TCE dose on formation of DAL protein adducts (A) and expression of CYP2E1

(B) in lung microsomes from TCE-treated CD-1 mice. Mice were treated with TCE at doses

ranging from 250-1000 mg/kg and were sacrificed 4 h after treatment. Control mice were treated

with corn oil. Lung microsomal proteins were separated by SDS-PAGE, transferred to a

membrane and stained with Ponceau S (C). The microsomal proteins were probed with an anti-

DAL antibody, the membrane was stripped and re-probed with an anti-CYP2E1 antibody. A

major band of 51 kDa was detected for both the DAL protein adduct (A) and CYP2E1 (B). Lanes

1 and 2: control; lane 3: 250 mg/kg; lane 4: 500 mg/kg; lane 5: 750 mg/kg; lane 6: 1000 mg/kg

TCE.

Fig. 5. Effect of TCE dose on formation of DAL protein adducts (A) and expression of CYP2F2

(B) in lung microsomes from TCE-treated CD-1 mice. Mice were treated with TCE (250, 500,

750 and 1000 mg/kg, i.p.) and were sacrificed 4 h after treatment. Control mice were treated

with corn oil. Lung microsomal proteins were separated by SDS-PAGE, transferred to a

membrane and stained with Ponceau S (C) to control for protein loading. The microsomal

proteins were probed with an anti-DCA antibody, the membrane was stripped and re-probed with

an anti-CYP2F1 antibody. A major band of 56 kDa was detected for both the DAL protein

adduct (A) and CYP2F2 (B). Lanes 1 and 2: control; lane 3: 250 mg/kg; lane 4: 500 mg/kg; lane

5: 750 mg/kg; lane 6: 1000 mg/kg TCE.

Fig. 6. Dose-dependent effects on rates of PNP hydroxylation in lung microsomes from TCE-

treated CD-1 mice. Mice were treated with TCE (50, 100, 250, 500, 750 and 1000 mg/kg, i.p.)

and were sacrificed 4 h after treatment. Reaction mixtures consisted of microsomal protein (0.5

mg) and NADPH (1.5 mM) in a total volume of 250 µl potassium phosphate buffer (100 mM),

pH 6.8, containing ascorbic acid (0.1 mM). Hydroxylation of PNP was estimated from

formation of 4-nitrocatechol and determined by HPLC analysis as described in *Materials and*

Methods. Data are expressed as mean ± S.D. of quadruplicate determinations.

Fig. 7. Dose-dependent formation of CH in incubations of TCE with lung microsomes from CD-

1 (A) and wild-type and CYP2E1-null mice (B). Reaction mixtures contained microsomal

protein (0.25 mg), NADPH (1.0 mM) and TCE (0-5.0   mM) in acetonitrile (0.4%, v/v) in a total

volume of 500 µl Tris-HCl buffer (50 mM), pH 7.4. Incubations were carried out for 20 min at

37°C. Levels of CH were determined by gas chromatography using the method described in

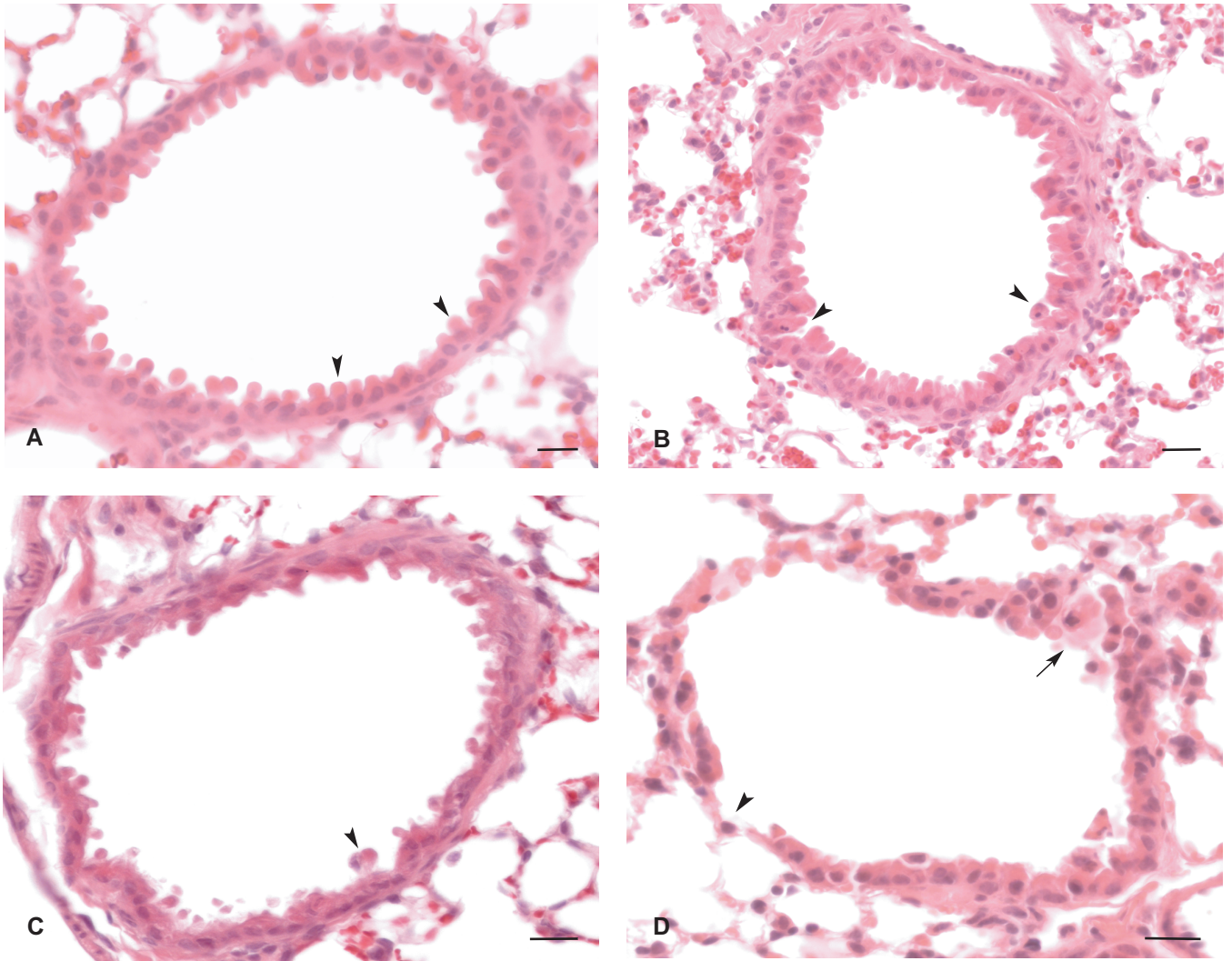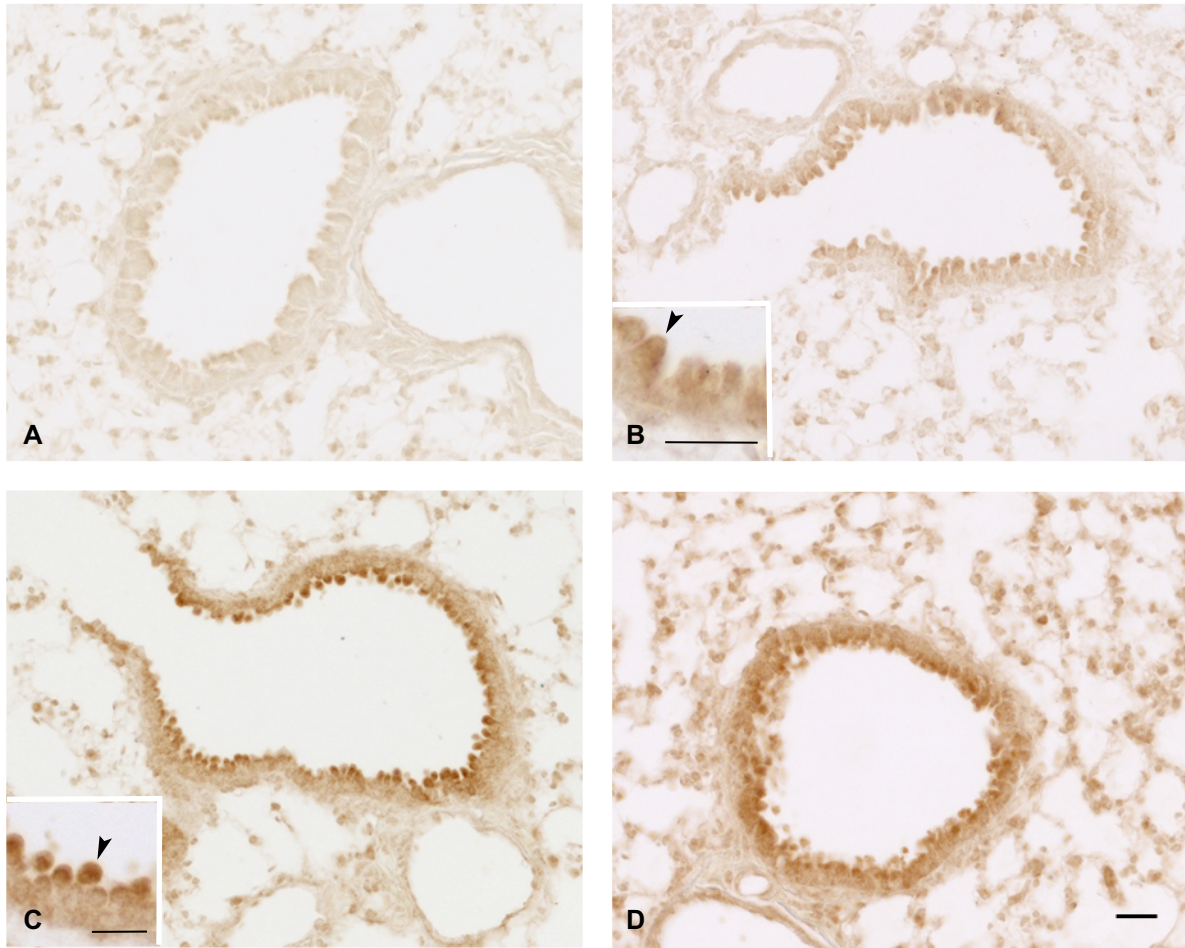*Material and Methods.* Data are expressed as mean ± S.D. of quadruplicate determinations.
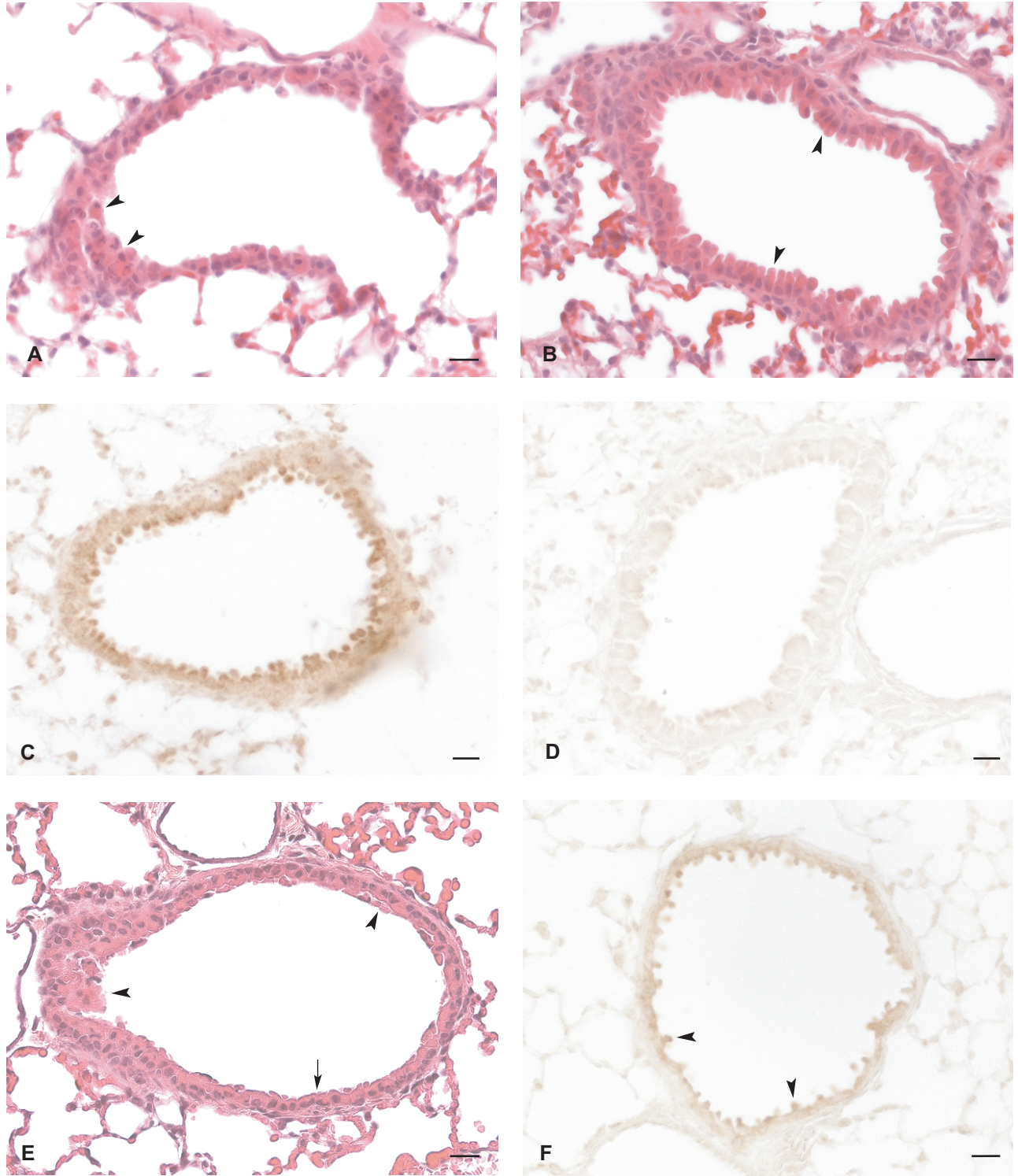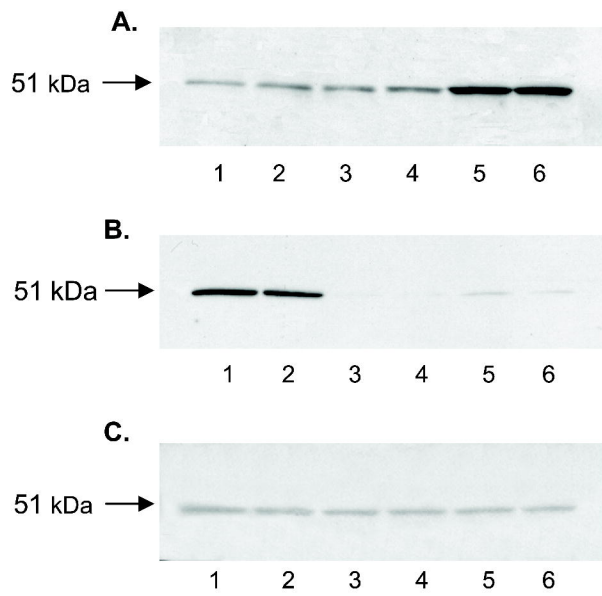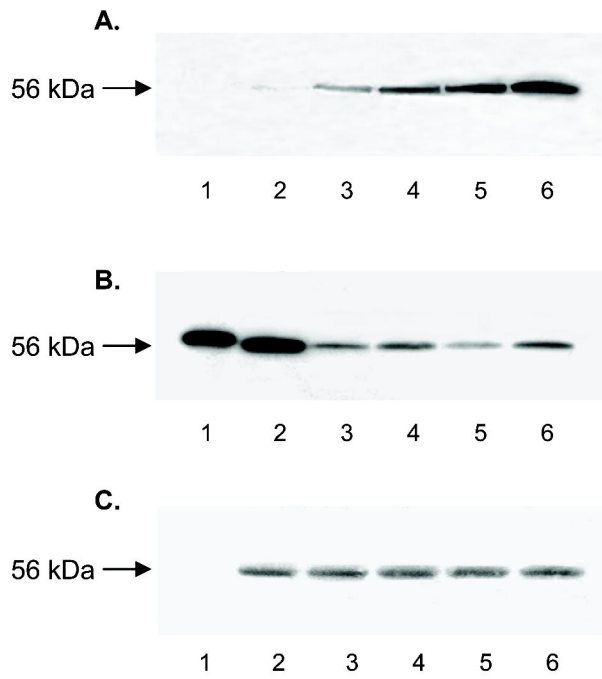
Figure 1

Figure 2

Figure 3

A.

51 kDa ⟶

    1   2   3   4   5   6

B.

51 kDa ⟶

    1   2   3   4   5   6

C.

51 kDa ⟶

    1   2   3   4   5   6

Figure 4

A.

56 kDa →

    1   2   3   4   5   6

B.

56 kDa →

    1   2   3   4   5   6

C.

56 kDa →

    1   2   3   4   5   6

Figure 5

Figure 6

A

B

Figure 7